3rd URSI AT-AP-RASC, Gran Canaria, 29 May – 3 June 2022

Modeling the radio wave polarization in transionspheric propagation

Kuldeep Pandey*(1), Robert G. Gillies(2), E. C. K. Eyiguler(1,3), Glenn C. Hussey(1), Donald W. Danskin(1), Andrew W. Yau(2)

(1) ISAS, Department of Physics and Engineering Physics, University of Saskatchewan, Saskatoon, Saskatchewan, Canada
(2) Department of Physics and Astronomy, University of Calgary, Calgary, Alberta, Canada
(3) Istanbul Technical University, Meteorological Engineering, Istanbul, Turkey

Abstract

The polarization characteristics of the radio waves traversing the ionosphere can be determined from the RRI (Radio Receiver Instrument) measurements onboard CASSIOPE/Swarm-E satellite. The rate of change of orientation angle of the HF radio waves indicate the Faraday rotation of the signal. A ray-trace model is used to simulate the radio wave orientation angle observed by the RRI. Input electron density profiles are constructed from the IRI (International Reference Ionosphere) model with the foF2 value scaled to the level measured by a nearby Digisonde. Results show that such IRI-model profiles closely reproduce the ionospheric electron density and help to model the radio wave orientation angle during transionospheric propagation.

1. Introduction

The transionospheric radio wave propagation is concerned with radio wave characteristics as it travels from the surface of the Earth into space or vice versa through the ionosphere. The dispersive nature of the ionosphere at high frequency (HF) causes the radio waves to propagate in two modes: the Ordinary (O-mode) and the Extraordinary (X-mode) [1]. As each mode has a slightly different refractive index in the ionosphere, the two modes have slight path differences. The corresponding difference in propagation time leads to an apparent rotation of the polarization ellipse that is known as Faraday rotation. For cross-dipoles the power appears to oscillate between the two dipoles and the polarization ellipse rotates as the wave propagates.

The CASSIOPE (CAScade, Smallsat, and Ionospheric Polar Explorer) satellite was launched into an elliptical (325-1,500 km), polar (81° inclination) orbit in September 2013. The Radio Receiver Instrument-RRI onboard the CASSIOPE/Swarm-E satellite provides the radio-wave polarization measurements. The rate of change of the orientation angle is an indicator of the Faraday rotation of the signal. Here, ray-tracing of HF radio waves is used to model the orientation angle changes in transionospheric radio wave propagation.

2. Dataset and ray-trace model inputs

The RRI uses two orthogonal 6-meter dipole antennas to provide the in-phase and quadrature components of the signal. The radio wave polarization characteristics were computed from the general Stokes parameters [2] using the complex voltages recorded on each dipole.

The present study examines the RRI observations of 21 December 2017. The RRI received 8.0995 MHz radio wave signals from the Ottawa HF transmitter (45.4°N, 75.6°W). The transmission alternated between continuous wave (CW) and binary phase shift keyed (BPSK) sequences [3]. The CW transmission started at each 10s boundary synchronized to UTC and continued for 0.9s. The BPSK sequence started 2s after every 10s boundary and the pattern was repeated every 15ms for 7s.

Geomagnetic conditions were quiet (Kp = 0) during the experiment. The F-region peak plasma frequency (foF2) and its altitude (hmF2) were obtained from ionograms of the Millstone Hill Digisonde (42.6°N, 71.5°W), about 500 km from Ottawa. The autoscaled foF2 and hmF2 values recorded on the ionograms were 2.675 MHz and 272 km respectively.

A three-dimensional ray-tracing program [4] was used to calculate the polarization orientation angle of the radio waves reaching the satellite. The model computes the propagation paths of radio waves from the Ottawa transmitter to the CASSIOPE satellite. The radio wave path is calculated based on the ray formalism of [5] and the Appleton-Hartree equation for the refractive index of radio waves in a magnetoionic medium. The input local geomagnetic field was taken from the International Geomagnetic Reference Field, IGRF model [6]. The input horizontally stratified electron density profiles were generated using the International Reference Ionosphere, IRI-model [7] with their maximum frequency adjusted to the observed foF2 value. At the endpoint of each radio wave path, the radio wave polarization was calculated based on the initial polarization of the wave, the overall propagation path, and the ending wave vector.

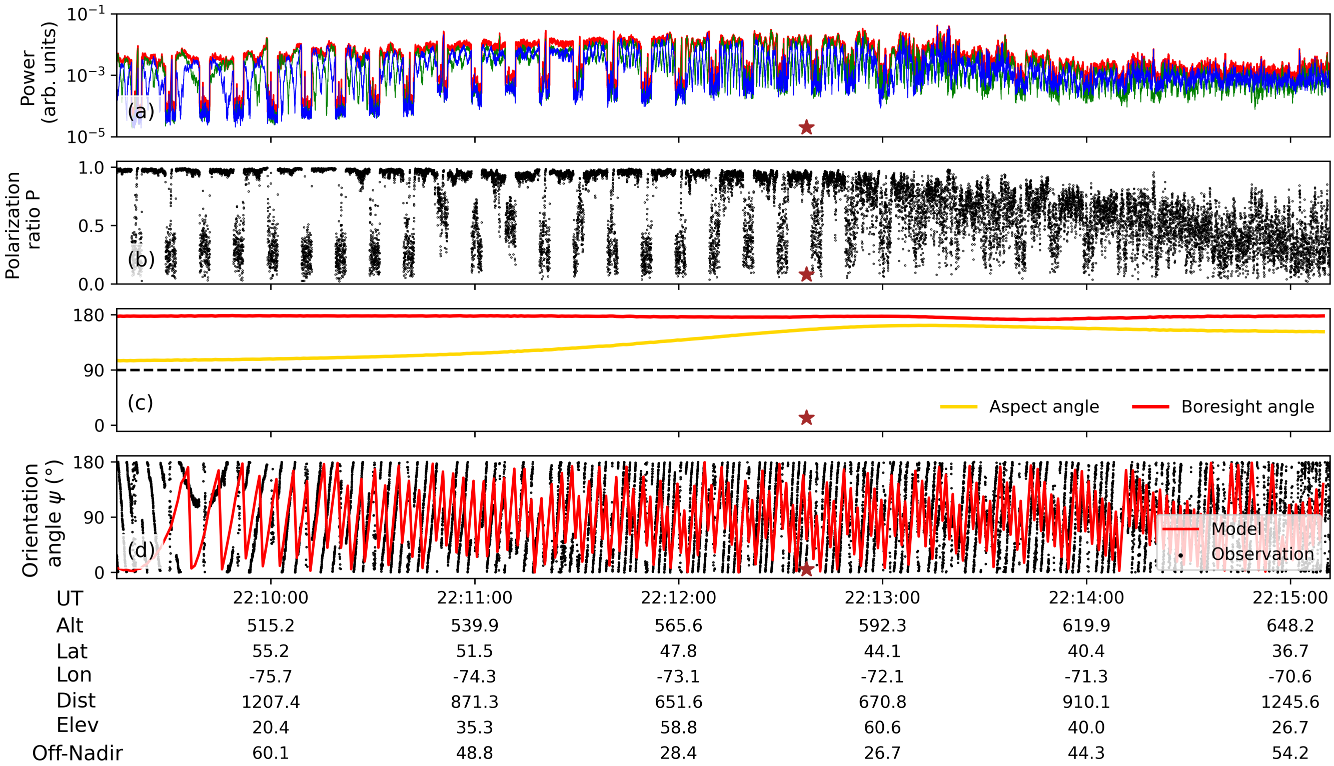

Figure 1. Transionospheric HF radio wave (a) power incident on RRI (green: dipole 1, blue: dipole 2, and red: total) and (b) Polarization ratio on the 21 December 2017 experiment. Panel (c) shows the calculated aspect angle of the signal (yellow) and the angle made by RRI boresight with the ray-vector (red). Panel (d) shows the observed (black) and modeled (red) orientation angle of the radio waves at the satellite location.

3. Results

Figure 1 shows the RRI based observation of radio wave characteristics and the ray-trace modeled orientation angle. Panel (a) shows the 15-ms average power received on the two dipoles (blue and green lines) along with their sum or total power (red line) of the radio wave signal incident on the RRI. The power plot shows the signatures of radio wave signals transmitted from the Ottawa transmitter at each 10-sec interval synchronized to UTC. The sharp reductions in power correspond to the dead-time between the CW and BPSK portions of repeat pattern. The abscissa of the bottom panel provides the satellite ephemeris and parameters from the Ottawa transmitter.

Figure 1(b) shows the Polarization ratio of the signals received by RRI. The high values (~1) show the signal intervals and coincide with the high levels of the total power. The polarization ratio drops when the transmitter was in one of the dead-time periods. Therefore, only the values with high power levels (at least three times the background level) are considered a signal for this paper.

Figure 1(c) shows the aspect angle (angle between the wave vector and geomagnetic field at the satellite location) with a yellow line. As the aspect angle varied in the range 105°-160°, the radio wave propagation had a mixture of quasi-transverse and quasi-longitudinal regimes. The boresight angle (angle between the RRI boresight and the wave vector at the satellite location) is shown by the red line. Since RRI was slewed towards Ottawa during this experiment, the offset angle remained close to 180° throughout the entire pass.

Figure 1(d) shows the 15-ms average orientation angle (black color dots) of the incident radio waves. The orientation angle changes in the full range from 0° to 180°, and the rate of change increases as the satellite travels from the north to the south of Ottawa (star symbol). The ray-trace modeled orientation angle values are shown by the red color. Broadly, the model and observed orientation angle show the same trend throughout the experiment. Both show that the rate of change of orientation angle increased from the north to the south of Ottawa. However, a direct comparison of the two values is not always possible due to their different temporal resolutions. The observed values have a 15-ms cadence. The model calculations are at a 1-sec cadence as the satellite ephemeris was only available once per second.

A reversal in the Faraday rotation was observed at ~21:09:40. The modeling shows this reversal occurring at ~21:09:15. The modeled orientation angle does not match completely the measurement, but the closeness indicates that only minor adjustments are needed to get better agreement.

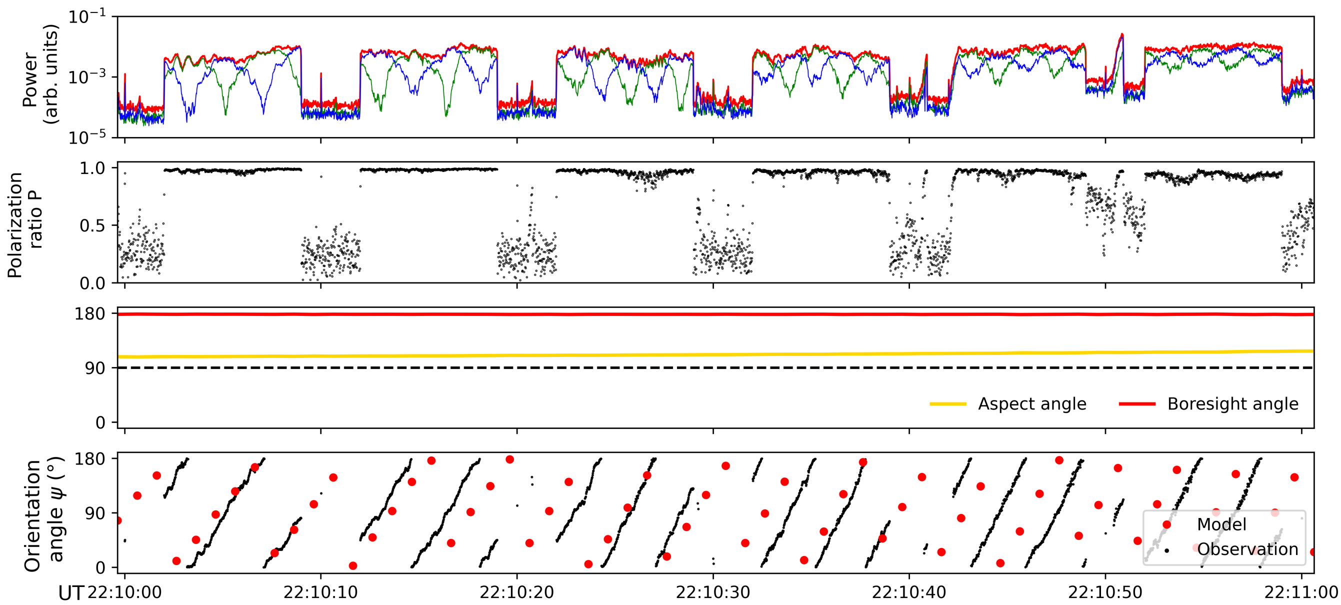

Figure 2. Same as Figure 1 but zoomed in for 1-min interval from 21:10:00 to 21:11:00 UT.

The slowest changes in orientation angle were at the beginning of the experiment. Therefore, a comparison between the modeled and observed orientation angle was possible at this time. Figure 2 shows the zoomed-in view of Figure 1 for the one minute interval (21:10:00 - 21:11:00 UT). The red dots in the bottom panel correspond to the modeled orientation angle at a 1-sec cadence. Both the modeled and observed orientation angle show the similar rate of change with small differences. Therefore, the ray-trace model captures the observed orientation angle behavior well.

4. Discussion

The results presented show that the orientation angle of radio waves could be modeled based on a ray-trace model. The inputs to the ray-trace model were the local geomagnetic field and ionospheric electron density. It is well known that the geomagnetic fields are stable and do not show a significant change on time scales of the order of a decade. However, the ionospheric density changes continuously with the hour of the day, season, and solar activity levels. Therefore, correctly providing the electron density profiles is extremely important to investigate the radio wave polarization during transionospheric propagation. The IRI-model was used for this purpose but with the foF2 value adjusted to the level measured by a nearby Digisonde. Once the foF2 levels were adjusted, the modeling appears to fit the measurements extremely well.

The profiles for the IRI-model seem to be very useful in the ray-tracing model. If the electron density profile was quite inaccurate, the ability to predict the rate of change of orientation angle would not be in good agreement over the wide range of latitude shown in Figure 1.

The offset in the Faraday reversal point between the observed and modeled orientation angle indicates that the modeling is quite near the necessary parameters. Adjusting the foF2 level should reduce the offset and would also give a better comparison in the 1-min interval as presented in Figure 2.

From Figure 2, the modeled points of orientation angle rarely fall near the extreme values of 0° and 180°. If the model was calculated at a temporal resolution finer than 1-sec, this apparent bias would disappear and the orientation angle would smoothly vary between 0° and 180°.

Similarly, later in the pass, the model and the measurement seem to fall apart. In actuality, the apparent disagreement is due to the resolution of the model. From the measurements, the orientation angle varied smoothly from 0° to 180° in about 1-sec. The model gives only one value at each second during which the satellite moves ~7 km, that is hundreds of wavelengths at the transmitter frequency of 8.099 MHz.

5. Summary

This paper summarizes the result of ray-tracing done for many passes of the CASSIOPE/Swarm-E satellite over the HF transmitter in Ottawa. One example has been presented in detail that shows how well the modeling agrees with observed data.

The modeling uses IGRF as a background geomagnetic field model. The IRI profile for the time of satellite experiment is used with the maximum density matched to the foF2 measured at Millstone Hill Digisonde. Small changes to the maximum density result in a much closer fit of the model to the measured data.

In general, for quiet geomagnetic conditions and for satellite passes where the RRI boresight slew-to-target, the modeled orientation angle agrees very well with the measurements. Adjustments of the foF2 usually are not much more than 1 MHz to provide good agreement with the orientation angle.

6. Acknowledgements

The CASSIOPE satellite measurements were taken from e-POP dataset (https://epop-data.phys.ucalgary.ca/). The Millstone Hill ionogram was taken from Digital Ionogram Database (https://ulcar.uml.edu/DIDBase/). Geomagnetic activity index Ap was obtained from World Data Center for Geomagnetism, Kyoto (http://wdc.kugi.kyoto-u.ac.jp/).

We gratefully acknowledge the funding support from the European Space Agency, MacDonald Dettwiler and Associates, the Canadian Space Agency, the Industrial Technologies Office and the Natural Science and Engineering Research Council (NSERC) for the development of the CASSIOPE mission, and operation of the CASSIOPE spacecraft, including the Cascade and e-POP payloads. Specifically, we acknowledge the support of the CSA [16SUSTTPHF] for the present study.

References

[1] *K. Davies, "Ionospheric radio", Peregrinus, 1990.*

[2] *M. Born, and E. Wolf, "Principles of optics: Electromagnetic theory of propagation, interference and diffraction of light", 6th Ed., Pergamon Press, 1980.*

[3] *D. W. Danskin, G. C. Hussey, R. G. Gillies, H. G. James, D. T. Fairbairn, and A. W. Yau, "Polarization characteristics inferred from the radio receiver instrument on the enhanced polar out flow probe", Journal of Geophysical Research: Space Physics, 123 (2), 2018, pp. 1648-1662, doi:10.1002/2017JA024731*

[4] *R. G. Gillies, G. C. Hussey, H. G. James, G. J. Sofko, and D. Andre, "Modelling and observation of transionospheric propagation results from ISIS II in preparation for ePOP", Annales Geophysicae, 25 (1), 2007, pp. 87-97, doi:10.5194/angeo-25-87-2007*

[5] *J. Haselgrove, "The hamiltonian ray path equations", Journal of Atmospheric and Terrestrial Physics, 25 (7), 1963, pp. 397-399, doi:10.1016/0021-9169(63)90173-9*

[6] *S. Maus, S. Macmillan, …., and T. Zvereva, "The 10th-Generation International Geomagnetic Reference Field", Geophysical Journal International, 161 (3), 2005, pp. 561-565, doi:10.1111/j.1365-246X.2005.02641.x*

[7] *D. Bilitza, D. Altadill, V. Truhlik, V. Shubin, I. Galkin, B. Reinisch, and X. Huang, "International reference ionosphere 2016: From ionospheric climate to real-time weather predictions", Space Weather, 15 (2), 2017, pp. 418-429. doi:10.1002/2016SW001593*